Characterisation of mesoporous polymer films deposited using lyotropic liquid crystal templating

Florian Bender [a], Terry C. Chilcott [b], Hans G.L. Coster [b],
D. Brynn Hibbert [a], J. Justin Gooding [a,*]

[a] *School of Chemistry, The University of New South Wales, Sydney, NSW 2052, Australia*
[b] *Biophysics and Bioengineering, Department of Chemical Engineering, The University of Sydney, Sydney, NSW 2006, Australia*

Abstract

Porous polymer films show interesting properties as ion selective membranes. In this work, poly(1,2-diaminobenzene) and polytyramine were deposited from hexagonal liquid crystal templates using two different surfactants. Resulting films were investigated to find evidence of mesoporous structures. While templated poly(1,2-diaminobenzene) has already been described as charge selective in the past, electrochemical experiments in this work demonstrate that another mechanism (most likely, size selectivity) also contributes to its ion selective behaviour. Films were characterised using spectroscopic ellipsometry and impedance spectroscopy. Results provide further evidence for the porosity, thinness, and the presence of ions in the templated poly(1,2-diaminobenzene) films. It is demonstrated that the use of a low-cost surfactant (Brij 56) is sufficient for the templating process. In contrast, polytyramine gave no evidence of being templated by the liquid crystal.
© 2006 Elsevier Ltd. All rights reserved.

Keywords: Liquid crystal templating; Mesoporous; Diaminobenzene; Charge selectivity; Size selectivity

1. Introduction

In recent years, great progress has been made in the field of nanofabrication. Many types of nanostructures have been created, among them porous films structured on a nanometre scale [1]. One of the interesting characteristics of these films is their ion selective behaviour which will be governed by their respective pore structure. Among the many materials and pore sizes that have been investigated, this work focuses on the fabrication of mesoporous polymer films (IUPAC defines the width of a mesopore as 2–50 nm). Until recently, fabrication of porous structures on the meso scale still proved particularly challenging [2].

A versatile method to produce periodic structures on a scale of about 1.5–30 nm is by templating using lyotropic liquid crystals [2–4]. Many surfactants, when mixed with water in the appropriate concentration range, will form lyotropic liquid crystal phases. Most interesting for this work is the hexagonal liquid crystal (H_I) phase where the surfactant molecules aggregate into parallel rods arranged in a hexagonal pattern, see Fig. 1a. The interior of the surfactant rods is hydrophobic while the aqueous component resides in the interspaces between individual rods. When a compound is electrodeposited from the aqueous component, a film with regular, well-defined openings may be formed, see Fig. 1b.

A family of surfactants suitable for this purpose are polyoxyethylene alkyl ethers many of which form H_I phases with water [5]. By varying the lengths of the alkyl (and polyoxyethylene) chains of the surfactant, the diameter of the surfactant rods and, consequently, the diameter of the openings in the resulting film can be varied. Furthermore, by adding a hydrophobic component (such as heptane) to the mixture that will dissolve in the interior of the surfactant rods, the openings can be made even larger [2,3,6].

Lyotropic liquid crystal templating was initially used to produce porous silicate which acts as a molecular sieve [2,3,7]. Further work extended the same templating strategy to other materials such as metal oxides [8,9], metal sulfides [10,11], and metals [6,12]. A breakthrough in this area was made by Attard et al. when they reported the application of liquid crystal templating
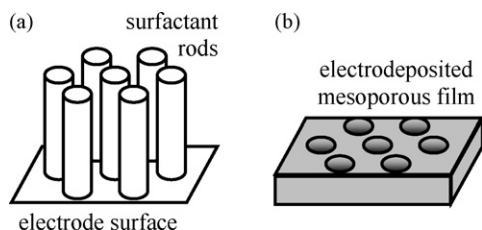
Fig. 1. (a) Schematic of the H_I liquid crystal phase. The case of orientation of the surfactant rods perpendicular to an adjacent electrode surface is shown. (b) Schematic of a film deposited in the presence of the liquid crystal (after subsequent removal of the surfactant).

via electrodeposition of a species in the aqueous phase of the liquid crystal [6]. In the first example, templating of platinum films of outstanding long-range order and considerable thickness (>1 μm) was achieved [6]. Subsequently using electrodeposition, very high surface roughness values (exceeding 3600) and, consequently, very high electrical capacitance values have been reported for mesoporous nickel [13]. The groups of Attard and Bartlett have also succeeded in templating films of various metals [14–18], non-metals [19,20], and a polymer [21] in this way.

The fabrication of mesoporous, non-conducting polymer films by liquid crystal templating is of particular interest because many ions will only be able to access the electrode through the nanometre-sized pores, and the latter will determine the permselective behaviour of the film. Electrodeposition is a potentially powerful way of fabricating such polymer films as the exquisite control over the amount of charge passed in an electrochemical process gives a high level of control over the thickness of polymer films. Varying the pore diameter as described above will then allow adjustment of the film properties for a particular application [21]. It has long been a major goal to engineer channels and pores with specific transport properties, such as charge and size selectivity [22]. In biology, the porous cell membrane is assumed to have a certain charge selectivity to prevent anions from leaking out [23]. Much research has been undertaken to use or mimic the characteristics of biological membranes to design channels and pores for biosensing and other applications [22–24]. The possibility to adjust the size of mesopores in liquid crystal templating provides a promising tool to control the size selectivity of the pore. In addition, a Donnan exclusion effect has been observed for liquid crystal templated films, providing them with charge selectivity [21,25].

The fabrication of bulk samples of a mesoporous polymer has also been reported [26]. In this case, the micellar phase of a mixture of surfactant and monomer solution was used as a template. Various applications have been proposed for the resulting mesoporous polymer (catalyst supports, double-layer capacitors, nanoreactors, adsorbents, optical devices, and supercapacitors) [26].

A polymer whose characteristics appear quite advantageous for the purpose of this work is poly(1,2-DAB) where DAB = diaminobenzene. It has been reported that electropolymerization of this polymer under the right conditions leads to ultra-thin but self-sealing, non-conducting, non-ionic films which show very little water uptake [27–29]. Evidence has been

found that this polymer is suitable for lyotropic liquid crystal templating [21]. It has been proposed that the mechanism of electropolymerization of poly(1,2-DAB), after initial formation of a monocation radical, proceeds by formation of amine linkages to the 4,5-positions of the next DAB molecule [30,31]. This is in contrast to the mechanism proposed by Lakard et al. for poly(1,4-DAB) which involves the elimination of an NH_2 radical, leading to a single amine linkage between adjacent phenyl rings [32].

Because of its promising characteristics, poly(1,2-DAB) was selected for this study. In addition, polytyramine (poly[4-hydroxyphenethylamine]) was investigated for comparison. Polytyramine is interesting for biosensing applications because the ethylamine group located at each phenyl ring can be exploited for the attachment of biological molecules such as proteins [33–35]. Electropolymerization of polytyramine has been reported to proceed only through the hydroxyl group of tyramine, forming ether bonds between adjacent phenyl rings and leaving the amine groups free for reproducible and stable enzyme attachment [36]. For this work, both polymers were deposited in liquid crystal-templated and non-templated form and investigated using various analytical techniques. Results are discussed with emphasis on the insight they give into the structure of the templated polymer films and on the potential the films show for biosensing and other analytical applications.

2. Experimental

2.1. Materials

The monomers selected as precursors for the polymer films were 1,2-DAB (specified ≤ 0.1% sulfated ash, supplier: Hopkin & Williams) and tyramine (purity 99%, Aldrich). Surfactants used were $C_{16}EO_8$ (octaethylene glycol monohexadecyl ether; 98%, Fluka) and Brij 56 (a mixture of poly(ethylene glycol) monohexadecyl ethers with average composition $C_{16}EO_{10}$, Sigma). The following compounds were used for electrochemical characterisation: potassium ferricyanide (99%, May & Baker); hexaammineruthenium(III) chloride (98%, Aldrich); and tris(1,10-phenanthroline) cobalt(II) tetrafluoroborate trihydrate which was synthesized in-house according to the procedure given by Dollimore and Gillard [37] but using tetrafluoroborate as the counterion instead of perchloric acid.

In addition, the following chemicals were used: H_2SO_4 (95–98%, Univar); KCl (99%, Sigma–Aldrich); and D_2O (99.9%, Cambridge Isotope Laboratories). H_2O was deionized and filtered using a Millipore Milli-Q system. Phosphate buffer was mixed in-house and consisted of 58 mM K_2HPO_4, 42 mM KH_2PO_4, and 0.1 M KCl dissolved in H_2O. Tris buffer was made by dissolving 50 mM tris(hydroxymethyl) aminomethane in H_2O and adjusting the pH to 7 using HCl; 0.5 M KCl was added for the experiments.

2.2. Liquid crystal preparation

The aqueous monomer solution was thoroughly mixed before adding the surfactant. For Brij 56, after adding a stirring bar, the

vessel was sealed and heated above the transition temperature of the liquid crystal phase to obtain a low viscosity. The mixture was then stirred until the entire sample was homogeneous. When $C_{16}EO_8$ was used as surfactant only a small amount of sample (30–100 μl) was prepared. In this case, after adding the surfactant, the sample was mixed manually using a spatula and a small vessel made for this purpose; care was taken to minimize the generation of bubbles in the sample.

2.3. Liquid crystal characterisation

Selected samples were characterised by ^{1}H NMR using a Bruker DPX 300 instrument. For these measurements, a mixture of 10% D_2O/90% H_2O was used for the monomer solution. The liquid crystal sample was heated and poured into a standard 10 mm NMR tube. The quadrupolar splitting of the deuterium peaks was recorded as a function of sample temperature. The anisotropic order of the H_I phase induces a splitting of the deuterium peak with peak separation of about 5 ppm or slightly more. Other phases show a different peak separation or no peak splitting at all.

For the samples containing 1,2-DAB and $C_{16}EO_8$, the phase was characterised using a microscope (Olympus BX 51) with heating stage (Linkam PE 120). For this purpose, a small amount of the sample (30–50 μl) was sandwiched between a microscope slide and a coverslip and placed between crossed polarisers. The sample was scanned visually for characteristic optical textures to identify the phase as a function of temperature [38].

2.4. Film deposition

Ten millimolar of the respective monomer was dissolved in phosphate buffer. For the non-templated polymer films, the film was deposited from this solution; for the templated polymer films, the monomer solution was mixed with either 45% (w/w) $C_{16}EO_8$ or 50% (w/w) Brij 56. Films were electrodeposited from the respective sample using a Solartron 1285 potentiostat by cycling 15 times between 0 and +1 V at a scan rate of 50 mV/s. If not otherwise stated, the working electrode was a 1 mm diameter gold disk electrode. The latter was polished prior to electrodeposition using a succession of alumina slurries (5 μm/1 μm/0.3 μm/0.05 μm particle sizes; Buehler) and a microcloth (Buehler) and cleaned by voltammetric cycling in 50 mM H_2SO_4 between −0.3 and +1.5 V until a repeatable cyclic voltammogram was obtained. A Pt gauze counter electrode and Ag/AgCl reference electrode were used. All electrodes were fabricated in-house. After film deposition, the working electrode was soaked in H_2O for 2 days with stirring to remove surfactant and other soluble material. The water was replaced every 2 h except overnight.

2.5. Electrochemical characterisation

Polymer films were characterised by voltammetric cycling in ferricyanide solution (5 mM potassium ferricyanide and 0.5 M KCl in H_2O; scan range −0.2 to +0.5 V), ruthenium hexaammine solution (5 mM hexaammineruthenium(III) chloride and 0.5 M

KCl in H_2O; scan range −0.6 to +0.1 V), or cobalt phenanthroline solution (5 mM tris(1,10-phenanthroline) cobalt(II) tetrafluoroborate trihydrate in tris buffer containing 0.5 M KCl; scan range −0.3 to +0.4 V). Characterisation was carried out using the Solartron 1285 potentiostat with a scan rate of 5 mV/s.

2.6. Spectroscopic ellipsometry

For ellipsometry, poly(1,2-DAB) films were deposited on pieces (about 1 cm²) of microscope slides, coated with 7 nm Cr and 100 nm Au by sputter coating. For templated films, Brij 56 was used as a surfactant. Films were characterised using a SOPRA GESP5 spectroscopic ellipsometer. Spectra were recorded for three different angles of incidence (55°/60°/65°). The wavelength range between 400 and 800 nm was selected for data analysis which was performed using WinElli 4.08 software. Since the exact optical properties of the polymer are unknown, a model was used to fit the data where three different layers represented the Cr, Au, and a generic polymer with an unknown percentage of void pore volume. Free parameters in the fitting procedure include the thicknesses of the Cr and Au layers and the percentage of void pore volume in the polymer, but for the analysis below results are represented only by the values for thickness and refractive index of the polymer at 632.8 nm.

2.7. Impedance spectroscopy

The impedance of the polymer films on the gold electrodes immersed in 0.1 M KCl was measured over a frequency range of about 10^{-2} to 10^5 Hz using a custom built impedance spectrometer with a resolution of 0.001° for the phase angle and 0.002% for the amplitude. The spectrometer applies a digitally generated sine wave alternating current, and the ac potential developed across the electrodes is monitored using high input impedance amplifiers. Details of the impedance spectroscopy system have been described previously [39–42].

For film characterisation, a pair of identical polymer-coated electrodes were placed in the 0.1 M KCl solution. While impedance measurements were performed for two identical polymer films in series, results were calculated for a single film at each electrode. The set-up with two coated electrodes in series was selected because for the thin polymer films only a small contribution in resistance was expected for most of the frequency range. The two films in series will double this effect. At least three complete impedance spectra were obtained for each system. As the spectrometer yields separate and precise measurements of the phase angle and impedance magnitude, the impedance at each frequency can be decomposed into an equivalent parallel combination of a capacitance and a conductance.

3. Results and discussion

A binary mixture of Brij 56 and water needs to be heated slightly above room temperature to obtain an H_I phase. At 30 °C the H_I phase extends from about 43.5–57% (w/w) surfactant [43]. Therefore, it was decided to mix the respective monomer

solution with 50% (w/w) Brij 56. When the monomer solution (10 mM in phosphate buffer) was used instead of water, the resulting mixture was already in H$_I$ phase even at room temperature (20 °C) for both monomers investigated. In the case of 1,2-DAB, a transition temperature from H$_I$ to micellar phases of 50 °C (±1 °C) was found by NMR, about 17 °C lower than that reported for the binary mixture [43]. Factors contributing to these differences might include the presence of the buffer salts and monomers as well as slight variations in the composition of Brij 56 from sample to sample. In the case of tyramine, a transition temperature from H$_I$ to micellar phases of 48 °C (±1 °C) was found.

For C$_{16}$EO$_8$, the binary phase diagram shows an H$_I$ phase for surfactant concentrations between about 37 and 68% (w/w) at room temperature [44]. Based on these figures, the respective monomer solution was mixed with 45% (w/w) C$_{16}$EO$_8$. For 1,2-DAB, the phase was determined using optical microscopy and identified as H$_I$ phase for the temperature range from 20 °C to the transition temperature of 54.5 °C (±1.5 °C). The latter is just slightly lower than that reported for the binary mixture.

Poly(1,2-DAB) was electrodeposited onto gold disk electrodes from buffer solution and from two different liquid crystal templates containing 45% C$_{16}$EO$_8$ and 50% Brij 56, respectively. Taking into account the smaller electrode surface in this work, the cyclic voltammograms (CVs) for buffer solution and C$_{16}$EO$_8$ look similar to those reported by Elliott et al. [21]. For the Brij 56 template, the CV still has a shape similar to that for C$_{16}$EO$_8$; however, the current during deposition was about a factor of 2 smaller for Brij 56. The following experiments were performed in order to find out if the lower current for Brij 56 has any detrimental effect on the characteristics of the resulting films.

It has been demonstrated previously that electrodes coated with C$_{16}$EO$_8$ templated poly(1,2-DAB) show charge selectivity when cycled in ferricyanide (negative ion) and ruthenium hexaammine (positive ion) solutions [21]. Fig. 2 shows the behaviour of electrodes coated with Brij 56 templated poly(1,2-DAB). While the electrochemistry in ferricyanide solution is blocked significantly for the electrode coated with the templated film, the same electrode behaves almost like a blank electrode in ruthenium hexaammine solution. The C$_{16}$EO$_8$ template yielded similar characteristics (not shown), despite the difference in current during film deposition from the two templates. This result indicates that the use of expensive, high-purity surfactants like C$_{16}$EO$_8$ is not a prerequisite for the fabrication of ion selective porous polymer films.

The ion selectivity described above has been discussed by Elliott et al. [21]. Since both ions are of similar size (0.5–0.8 nm), the effect has been attributed to the difference in charge. It was concluded that the templated poly(1,2-DAB) films contain negative charges, possibly in the form of encapsulated chloride ions. This would explain why positive ions can enter the pores while negative ions can only enter if a background electrolyte of very high concentration is present, thus counterbalancing the encapsulated charges. On the other hand, for non-templated poly(1,2-DAB) films deposited from acetate buffer, no incorporated ions were found [28,29]. These observations are consistent
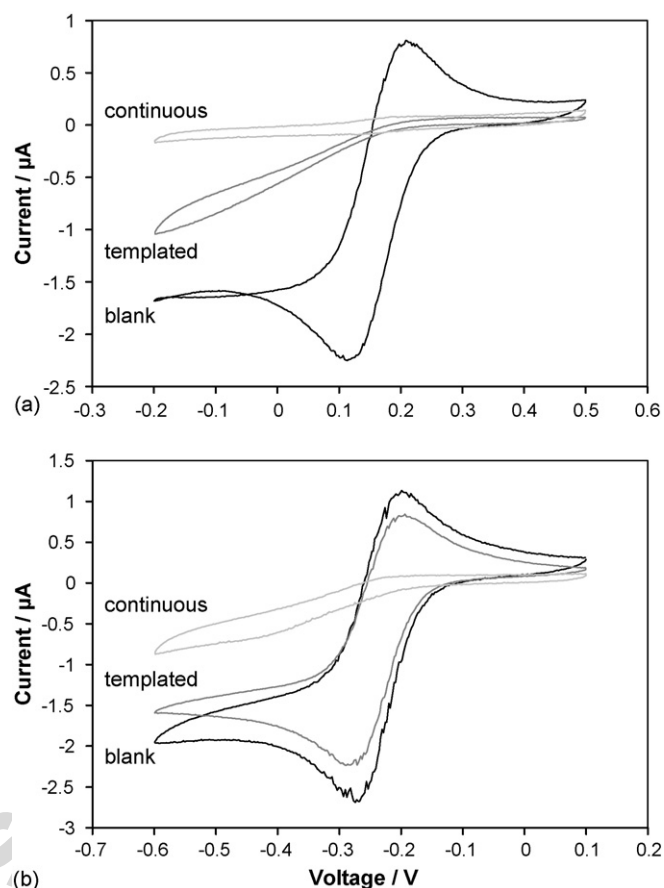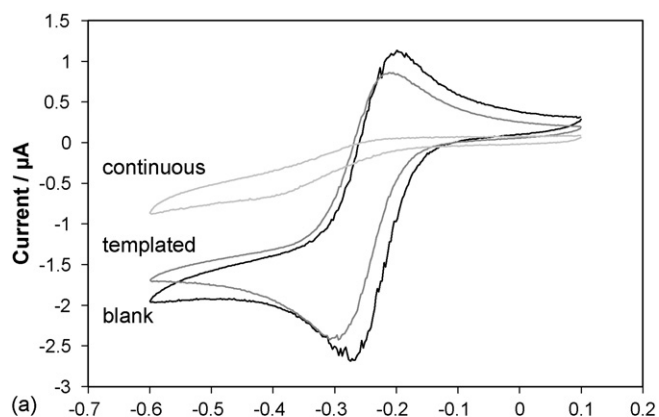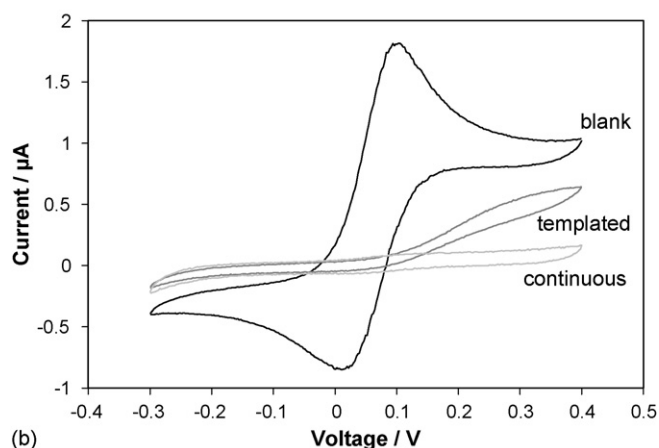

Fig. 2. CVs of various 0.79 mm^2 gold disk electrodes in 5 mM ferricyanide (a) and 5 mM ruthenium hexaammine (b). Electrodes are labelled "continuous" (non-templated poly(1,2-DAB) film), "templated" (Brij 56 templated poly(1,2-DAB) film), and "blank" (blank gold disk electrode). Scan rate, 5 mV/s.

with a Donnan exclusion effect which depends on the exact conditions of film deposition, e.g., the presence of chloride ions.

Polytyramine was also deposited onto gold disk electrodes from buffer solution and from the same two liquid crystal templates as for poly(1,2-DAB) and the ion selectivity of the resulting films was investigated. However, if polytyramine was cycled to the negative voltages needed for the redox chemistry of ruthenium hexaammine the films started delaminating. Therefore, cobalt phenanthroline was selected as the positive ion in this experiment since its redox chemistry takes place at nearly the same potential as that of ferricyanide. It was found that the electrochemistry of both ferricyanide and cobalt phenanthroline is blocked significantly in the case of polytyramine electrodeposited from the templating liquid crystal phase. A similar observation was made if the polytyramine films were deposited from Brij 56 instead of C$_{16}$EO$_8$. In both cases, the templated polytyramine films behaved just like the non-templated films. This suggests the liquid crystal templating mechanism failed to produce a mesoporous polytyramine film. However, an alternative explanation was the cobalt phenanthroline ion is significantly larger (1.22 nm) [45] than the other ions used in this work and hence the exclusion of the cobalt phenanthroline ion from any pores could also arise from a size selectivity effect. (In addition, it has been proposed that even specific chemical
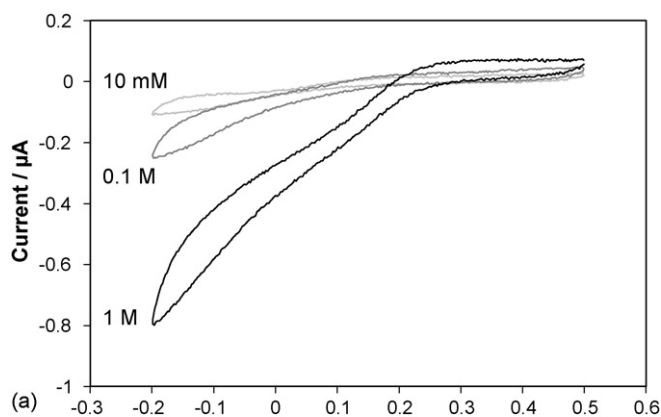
Fig. 3. CVs of various 0.79 mm² gold disk electrodes in 5 mM ruthenium hexaammine (a) and 5 mM cobalt phenanthroline (b). Electrodes are labelled "continuous" (non-templated poly(1,2-DAB) film), "templated" ($C_{16}EO_8$ templated poly(1,2-DAB) film), and "blank" (blank gold disk electrode). Scan rate, 5 mV/s.

Fig. 4. CVs of a 0.79 mm² gold disk electrode coated with $C_{16}EO_8$ templated poly(1,2-DAB) in 5 mM ferricyanide (a) and 5 mM cobalt phenanthroline (b). Respective concentrations of background electrolyte (KCl) are given in the figure. Scan rate, 5 mV/s.
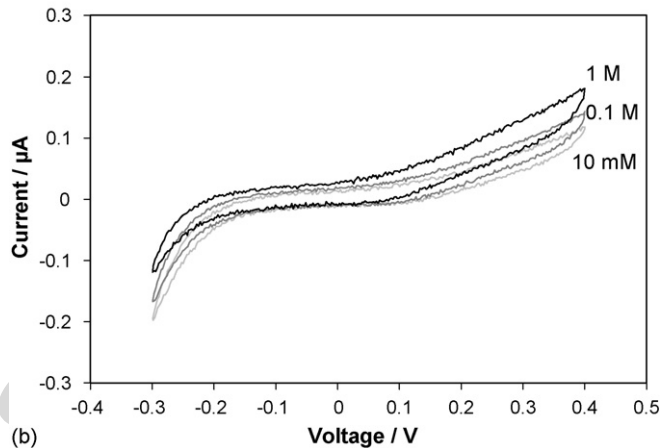
interactions like hydrophobic interaction or hydrogen bonding could also play a significant role in the permselective behaviour of poly(1,2-DAB) [28].)

To clarify this point, $C_{16}EO_8$ templated poly(1,2-DAB) films were characterised in ruthenium hexaammine and cobalt phenanthroline solutions. In the case of ruthenium hexaammine, the CV for the templated film is again similar to that of an uncoated electrode in ruthenium hexaammine (Fig. 3a). In contrast, in cobalt phenanthroline the electrochemistry for the templated poly(1,2-DAB) films is significantly suppressed relative to the bare electrode. Thus, it is still not clear whether the suppression of electrochemistry in the polytyramine film deposited from the templating solution is due to a lack of nanostructure or not. Prior to presenting other methods of characterisation to verify the structure of the polytyramine films, Fig. 3 warrants further discussion.

Although the suppression of the cobalt phenanthroline electrochemistry by the templated poly(1,2-DAB) films fails to clarify whether the templating was successful with polytyramine films, Fig. 3 suggests that the behaviour of the poly(1,2-DAB) films cannot be explained simply in terms of charge selectivity. Ruthenium hexaammine and cobalt phenanthroline are both cations, but only the former can readily pass through the pores.

The difference in size of the two ions could well explain these findings. However, to accept such an explanation an alternative hypothesis, that the exclusion could be related to the difference in their redox potentials changing the charge exclusion attributes of the polymer, must be discounted. To investigate this possibility electrodes coated with $C_{16}EO_8$ templated poly(1,2-DAB) films were characterised in ferricyanide and cobalt phenanthroline solutions, with varying concentration of background electrolyte (KCl). As Fig. 4a demonstrates, KCl concentration has a significant effect on the ability of the ferricyanide ions to pass through the pores, consistent with Donnan exclusion behaviour as discussed above. The same is clearly not the case for cobalt phenanthroline, see Fig. 4b. Therefore, charge selectivity can be ruled out in the case of cobalt phenanthroline, leaving size selectivity as the most likely reason for the exclusion of this species from the pores.

Further information about the structure of the templated polymer films can be obtained by subjecting the polymer-coated electrode to a second deposition process to fill any pores in the polymer film with additional polymer material. For this purpose, after deposition of the templated (or non-templated) polymer film the electrode was first rinsed in water for 2 days to remove the surfactant (and buffer), and then immersed in the monomer/buffer solution (without surfactant) and cycled again

Table 1
Optical thickness and refractive index at 632.8 nm for various non-templated and Brij 56 templated poly(1,2-DAB) films determined using spectroscopic ellipsometry

Film type	Thickness (nm)	Refractive index
Non-templated	14.2	1.90
	14.1	1.89
Templated	11.2	1.77
	11.8	1.62
	10.0	1.67

Nominal error values for the fitting procedure are about ±0.3 nm for the thickness and ±0.01 for the refractive index.

as described in Section 2. For non-templated poly(1,2-DAB), it has been demonstrated that no significant amount of polymer can be deposited on top of the film, indicating that after 2 days of rinsing in water the film is still intact and largely free of pores. This is consistent with the picture of a quite impermeable, pinhole-free film as described in literature [28,29]. In contrast, if a templated poly(1,2-DAB) film is subjected to a second deposition process, a significant amount of material will be deposited; further evidence the templated polymer has enhanced porosity. This result is consistent with previous work by Elliott et al. [21] who suggested the porosity of the templated poly(1,2-DAB) films was approximately 25%, as determined by comparing the charge passed in this second deposition with the charge passed when generating a non-templated film. Using the same approach, the templated films generated in the current study have a slightly higher porosity of approximately 30%.

For polytyramine, the same experiment gave very different results. Even on the non-templated polytyramine films, a significant amount of charge (about 10% of that of the non-templated film) could be deposited after rinsing for 2 days. This indicates either the presence of cracks or pinholes in the film, or the existing film has undergone changes so it can be partly re-oxidised. Even more significantly, the amount of charge that could be deposited on polytyramine films deposited from the templating solution was comparable to the case of the non-templated films, again indicating that in terms of their porosity there is no significant difference between the two. This is consistent with the hypothesis above that the templating mechanism fails in the case of polytyramine. Hence no further work was performed on polytyramine.

It has been reported before that the templated poly(1,2-DAB) films are extremely difficult to characterise physically [21]. XRD, TEM, and AFM have all failed in the past to produce consistent results for these films. In the present work, spectroscopic ellipsometry and impedance spectroscopy were used to further characterise the films.

Both non-templated and Brij 56 templated poly(1,2-DAB) films were analysed by spectroscopic ellipsometry. Results are summarised in Table 1. For non-templated films, the analysis (the procedure is briefly described in Section 2) gives values of 14.1 nm (±0.3 nm) for the thickness and 1.89 (±0.01) for the refractive index (here, error values reflect the nominal uncertainty of the fitting procedure rather than the scatter of the data). Both values are slightly higher than expected. For the thick-

ness, values of about 10 nm [28,29] or below 10 nm [21,27] have been reported in the literature. The refractive index of electrodeposited poly(1,2-DAB) as a function of wavelength was not known; however, similar polymers give values below 1.8 for the refractive index at 632.8 nm [46,47]. Given the simplifying assumptions made in the analysis, the results are still consistent with literature values and can certainly serve as a basis for comparison with the templated films.

For templated poly(1,2-DAB) films, a thickness of 11.0 nm (±0.9 nm) and a refractive index of 1.69 (±0.08) were obtained. It is interesting to note that the templated films are both considerably thinner and have a lower refractive index. The latter is consistent with the porosity found in the electrochemical experiments. They also exhibit a significant scatter in the data: a total of three measurements on two electrodes gave a standard deviation of 8.2 and 4.7% for the thickness and refractive index, respectively. This is most likely related to the high viscosity of the liquid crystal samples which allows local variations, e.g., in sample composition or orientation of the surfactant rods relative to the surface.

Impedance spectroscopy provides insight into the structure and properties of thin films by measuring the variation of electrical capacitance and conductance as a function of frequency [39–42]. For the type of thin films on gold that are the subject of this study, the dispersion in these parameters is most prominent at low frequencies (0.1–1000 Hz). Since for impedance spectroscopy measurements two identical polymer-coated electrodes were immersed together in the same solution (0.1 M KCl) and the current passed through both films in series, the values of conductance and capacitance of a single film at each frequency are simply twice the values for the series combination.

The conductance and capacitance measured as a function of ac frequency for a pair of gold electrodes coated with a non-templated film of poly(1,2-DAB) are shown in Fig. 5. For comparison, graphs for the same pair of gold electrodes before coating are also shown. The drop in both conductance and capacitance at low frequencies indicates the presence of the film. The curves of the capacitance as a function of frequency for the coated and uncoated electrodes cross over at a frequency of a few kHz. It should be emphasized that the plots in Fig. 5 are on a logarithmic scale. The differences, particularly in the capacitance, are therefore significant; even the differences in the conductance are substantial for frequencies exceeding 100 Hz. At frequencies above about 1 kHz, both the coated and uncoated electrodes show a dispersion that reflects the presence of the electrolyte solution between (i.e., in series with) the electrodes. This series resistance element (electrolyte conductance: 1.45 mS) can be readily subtracted from the complex impedance. This allows the remaining dispersion of conductance and capacitance of the system to be plotted on an expanded scale to highlight differences between coated and uncoated electrodes, as shown in Fig. 6. While the conductance of the electrode coated with non-templated poly(1,2-DAB) is significantly lower than that of the uncoated electrode, the conductance (particularly at frequencies above 1 kHz) is still higher than what might be expected from an ideal polymer film with no defects, as detailed below.
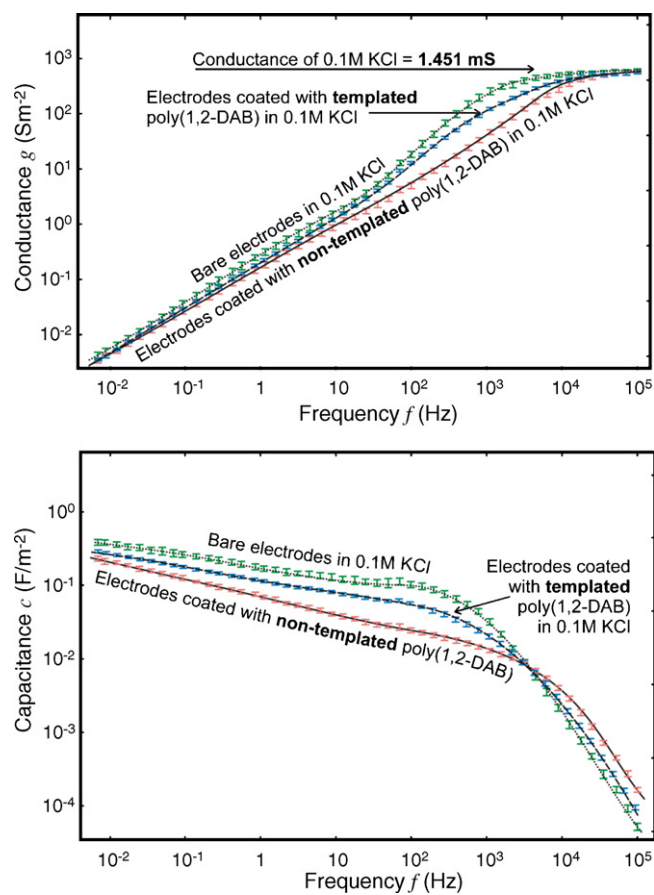
Fig. 5. Conductance and capacitance as a function of frequency for a pair of 0.79 mm^2 gold disk electrodes either uncoated or coated with C$_{16}$EO$_8$ templated or non-templated poly(1,2-DAB) as indicated in the graph. Electrodes were immersed in 0.1 M KCl.

Fig. 6. Conductance and capacitance of the uncoated gold electrodes and the C$_{16}$EO$_8$ templated and non-templated poly(1,2-DAB) films, respectively, after subtraction of the contribution of the conductance of the electrolyte in series with the electrodes. This allows the differences between the templated and non-templated films to be more readily discerned. The dispersion of the conductance and capacitance for the uncoated electrode now refers to the ionic double layer formed at the electrode–solution interface.

The dispersion with frequency of the conductance and capacitance of the polymer films on gold can be modelled, as a first approximation, by representing each film as a series combination of several layers of material with different dielectric properties, in series with the bare electrode. At high frequencies (above 100 Hz), the capacitance required to account for the contribution of the polymer film amounts to about 20 nF/m^2 for non-templated poly(1,2-DAB). For C$_{16}$EO$_8$ templated poly(1,2-DAB), the contribution is about 45 nF/m^2 (see Figs. 5 and 6). The conductance of the templated film for frequencies above 100 Hz was a factor of 2–3 higher than that of the non-templated film. However, the latter was still relatively high (about 40 kS/m^2), an indication that the films might contain trapped water and ions. In this case, it would be expected that the dielectric constants of the films would also be relatively high, much higher than that of bulk samples of the polymer. For an estimated dielectric constant of the non-templated film of about 30 and a roughness factor of 1.5 (± 0.3) for the electrode surface [48], the resulting thickness of the film would be near 10 nm. The capacitance of the templated film estimated from the series element it represents in the above approximation is a factor of 2.25 larger than that of the non-templated film. Based on this, and assuming a similar or slightly lower thickness for the templated film, the dielectric constant of the latter would be estimated to be around 60, indicating a
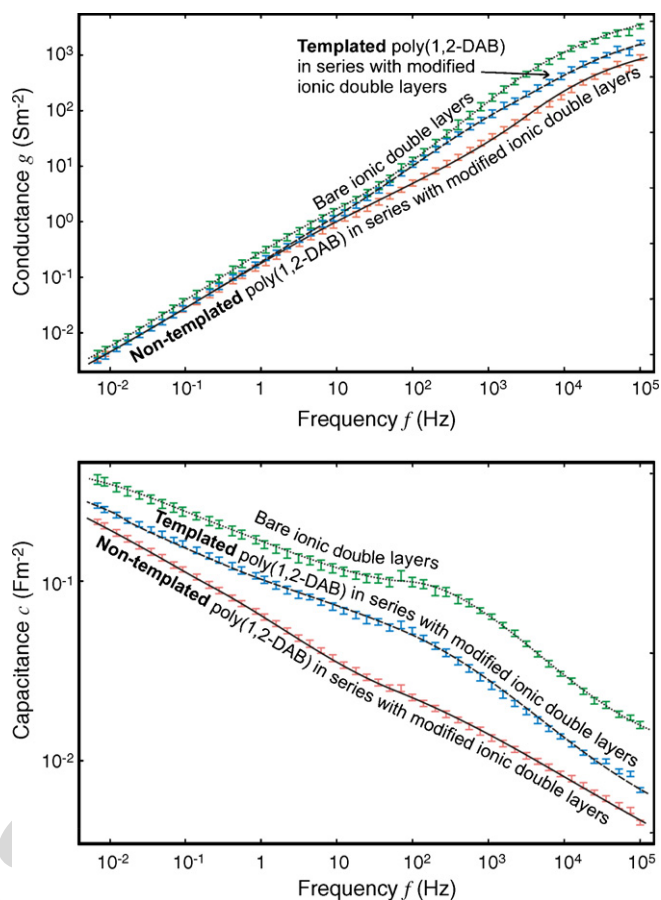
film permeated to a large degree by ions/electrolyte solution. It should be noted that these findings do not contradict the estimate for the porosity made above since it has been suggested that the films contain *encapsulated* ions [21], in addition to the electrolyte solution contained in the pores.

Another point that should be mentioned here is that calculating the capacitance of the film from the difference in capacitance between the bare electrode and the coated electrode makes the implicit assumption that the ionic double layer and hence the capacitance of the interface at the gold electrode is not itself perturbed by the presence of the polymer film. Clearly, this is not likely to be the case.

At the gold–solution interface, ions are attracted to the gold surface due to electrostatic image forces (Born energy) which arise because the aqueous solution has a dielectric constant which is smaller than that of the gold (which effectively has an infinite dielectric constant). The presence of the polymer, which is a material of relatively low dielectric constant (compared to water), would be expected influence this ionic "double" layer, both through the modulation of the Born energy of ion adsorption and through changes in the Debye length (and hence thickness

of the double layer). The films permeated by the electrolyte to the extent suggested by the present results indicate that this perturbation may not be very great, particularly in the case of the templated films.

4. Conclusions

The combination of the electrochemical experiments performed clearly demonstrates that the two polymers investigated perform differently in liquid crystal templating. There is sufficient evidence to conclude that templated polytyramine is not mesoporous. On the other hand, voltammetric cycling in various electrolytes, impedance spectroscopy, spectroscopic ellipsometry and re-deposition of polymer on top of a templated film all indicate a significant porosity for the templated poly(1,2-DAB) films. The question arises why the two polymers behave differently. It is not a foregone conclusion that polytyramine never forms any pores in the templating process. Alternatively, a meso-pore structure might be formed temporarily but the polymer film might relax after surfactant removal, resulting in the loss of the pore structure. To prevent this, the polymer film must be fairly rigid (or largely free of stress). Poly(1,2-DAB) has two amine bonds between neighbouring phenyl rings, resulting in about twice the charge transfer during film deposition compared to polytyramine. This rigid molecular structure, together with its low water uptake [28], might help to provide poly(1,2-DAB) with the ability to preserve the mesopore structure after surfactant removal. Many other polymers, due to the high degree of mobility in their molecular structures, might not have this ability.

A comparison of the results from impedance spectroscopy with those from ellipsometry (and literature) [21,27–29] gives high estimates for the dielectric constants of the poly(1,2-DAB) films. These results are based on simplifying assumptions made in the analysis as discussed above. However, taking into account the charge selectivity of templated poly(1,2-DAB), there is nevertheless strong evidence of trapped ions (and water) in the films. It should be noted that the trapped ions do not necessarily reflect the bulk properties of the electrolyte present during film deposition. Since the polymer films are so thin, surface effects must be considered. The presence of the ionic double layer, concentration gradients (a voltage of up to +1 V is applied during film deposition), and other physical or even chemical effects might play a role. Therefore, the results of this study reflect not only the properties of the polymer materials investigated but also the influence of the surface processes taking place during electrodeposition.

The measured thicknesses of the films are consistent with literature values (about 10 nm), within the uncertainty of the measurement. Spectroscopic ellipsometry indicates the templated films are thinner than the non-templated films by about 20–25%. Impedance spectroscopy yields capacitances (and conductances) for the templated films much larger than those of the non-templated films. This is consistent with the results from spectroscopic ellipsometry because both the higher porosity (and, therefore, higher dielectric constant) and lower thickness of the templated films are expected to result in an increase in capacitance and conductance.

Templated poly(1,2-DAB) also stands out from the other films investigated due to its ion selectivity. While it was concluded that (negative) ferricyanide ions are excluded from the pores of this polymer by a charge selectivity effect [21], the (positive) cobalt phenanthroline ion is excluded most likely by a size selectivity effect. This, together with the Donnan exclusion effect discussed above, indicates the existence of a preferential pore size, in agreement with the interpretation of the pore structure as a template of the liquid crystal phase.

Given the complex ion selectivity of templated poly(1,2-DAB) and the ease of its fabrication, this mesoporous film can be a useful element in biosensing and chemical sensing applications. The experiments above demonstrate its general suitability for ion sensors, and the ions used give a rough idea of its preferential pore size. Further work is needed to give a more precise idea of the pore size and the range of ions that can be detected.

Due to its well-defined pore structure, the film may also serve as an interesting platform for nano-assembly. It was demonstrated that a low-cost surfactant (Brij 56) is sufficient to template the ion selective poly(1,2-DAB) films. This is an important prerequisite for any commercial use of this templating process.

References

[1] C. Park, J. Yoon, E.L. Thomas, Polymer 44 (2003) 6725.
[2] J.S. Beck, J.C. Vartuli, W.J. Roth, M.E. Leonowicz, C.T. Kresge, K.D. Schmitt, C.T.-W. Chu, D.H. Olson, E.W. Sheppard, S.B. McCullen, J.B. Higgins, J.L. Schlenker, J. Am. Chem. Soc. 114 (1992) 10834.
[3] C.T. Kresge, M.E. Leonowicz, W.J. Roth, J.C. Vartuli, J.S. Beck, Nature 359 (1992) 710.
[4] D. Zhao, J. Feng, Q. Huo, N. Melosh, G.H. Fredrickson, B.F. Chmelka, G.D. Stucky, Science 279 (1998) 548.
[5] D.J. Mitchell, G.J.T. Tiddy, L. Waring, T. Bostock, M.P. McDonald, J. Chem. Soc., Faraday Trans. 1 (79) (1983) 975.
[6] G.S. Attard, P.N. Bartlett, N.R.B. Coleman, J.M. Elliott, J.R. Owen, J.H. Wang, Science 278 (1997) 838.
[7] G.S. Attard, J.C. Glyde, C.G. Goltner, Nature 378 (1995) 366.
[8] Q. Huo, D.I. Margolese, U. Ciesla, P. Feng, T.E. Gier, P. Sieger, R. Leon, P.M. Petroff, F. Schüth, G.D. Stucky, Nature 368 (1994) 317.
[9] P. Yang, D. Zhao, D.I. Margolese, B.F. Chmelka, G.D. Stucky, Nature 396 (1998) 152.
[10] P.V. Braun, P. Osenar, S.I. Stupp, Nature 380 (1996) 325.
[11] P.V. Braun, P. Osenar, V. Tohver, S.B. Kennedy, S.I. Stupp, J. Am. Chem. Soc. 121 (1999) 7302.
[12] G.S. Attard, S.A.A. Leclerc, S. Maniguet, A.E. Russell, I. Nandhakumar, B.R. Gollas, P.N. Bartlett, Microporous Mesoporous Mater. 44 (2001) 159.
[13] V. Ganesh, V. Lakshminarayanan, Electrochim. Acta 49 (2004) 3561.
[14] P.N. Bartlett, P.N. Birkin, M.A. Ghanem, P. de Groot, M. Sawicki, J. Electrochem. Soc. 148 (2001) C119.

[15] P.A. Nelson, J.M. Elliott, G.S. Attard, J.R. Owen, Chem. Mater. 14 (2002) 524.
[16] P.N. Bartlett, B. Gollas, S. Guerin, J. Marwan, Phys. Chem. Chem. Phys. 4 (2002) 3835.
[17] P.N. Bartlett, J. Marwan, Microporous Mesoporous Mater. 62 (2003) 73.
[18] A.H. Whitehead, J.M. Elliott, J.R. Owen, G.S. Attard, Chem. Commun. (1999) 331.
[19] I. Nandhakumar, J.M. Elliott, G.S. Attard, Chem. Mater. 13 (2001) 3840.
[20] T. Gabriel, I.S. Nandhakumar, G.S. Attard, Electrochem. Commun. 4 (2002) 610.
[21] J.M. Elliott, L.M. Cabuché, P.N. Bartlett, Anal. Chem. 73 (2001) 2855.
[22] H. Bayley, Curr. Opin. Biotechnol. 10 (1999) 94.
[23] S. Cheley, L.-Q. Gu, H. Bayley, Chem. Biol. 9 (2002) 829.
[24] E.D. Steinle, D.T. Mitchell, M. Wirtz, S.B. Lee, V.Y. Young, C.R. Martin, Anal. Chem. 74 (2002) 2416.
[25] J.M. Elliott, P.R. Birkin, P.N. Bartlett, G.S. Attard, Langmuir 15 (1999) 7411.
[26] J. Jang, J. Bae, Chem. Commun. 9 (2005) 1200.
[27] S.V. Sasso, R.J. Pierce, R. Walla, A.M. Yacynych, Anal. Chem. 62 (1990) 1111.
[28] D. Centonze, C. Malitesta, F. Palmisano, P.G. Zambonin, Electroanalysis 6 (1994) 423.
[29] F. Palmisano, P.G. Zambonin, D. Centonze, Fresenius J. Anal. Chem. 366 (2000) 586.
[30] W.R. Heineman, H.J. Wieck, A.M. Yacynych, Anal. Chem. 52 (1980) 345.
[31] D.-H. Jang, Y.-S. Yoo, S.M. Oh, Bull. Korean Chem. Soc. 16 (1995) 392.
[32] B. Lakard, G. Herlem, S. Lakard, B. Fahys, J. Mol. Struct. (Theochem) 638 (2003) 177.
[33] M. Situmorang, J.J. Gooding, D.B. Hibbert, Anal. Chim. Acta 394 (1999) 211.
[34] M. Situmorang, J.J. Gooding, D.B. Hibbert, D. Barnett, Electroanalysis 13 (2001) 1469.
[35] M. Situmorang, J.J. Gooding, D.B. Hibbert, D. Barnett, Electroanalysis 14 (2002) 17.
[36] M. Yuqing, C. Jianrong, W. Xiaohua, Trends Biotechnol. 22 (2004) 227.
[37] L.S. Dollimore, R.D. Gillard, J. Chem. Soc., Dalton Trans. (1973) 933.
[38] F.B. Rosevear, J. Am. Oil Chem. Soc. 31 (1954) 628.
[39] T.C. Chilcott, H.G.L. Coster, E.P. George, J. Membr. Sci. 100 (1995) 77.
[40] H.G.L. Coster, T.C. Chilcott, A.C.F. Coster, Bioelectrochem. Bioenerg. 40 (1996) 79.
[41] T.C. Chilcott, M. Chan, L. Gaedt, T. Nantawisarakul, A.G. Fane, H.G.L. Coster, J. Membr. Sci. 195 (2002) 153.
[42] L. Gaedt, T.C. Chilcott, M. Chan, T. Nantawisarakul, A.G. Fane, H.G.L. Coster, J. Membr. Sci. 195 (2002) 169.
[43] N.R.B. Coleman, G.S. Attard, Microporous Mesoporous Mater. 44–45 (2001) 73.
[44] G.S. Attard, P.N. Bartlett, N.R.B. Coleman, J.M. Elliott, J.R. Owen, Langmuir 14 (1998) 7340.
[45] D. ben-Avraham, L.S. Schulman, S.H. Bossmann, C. Turro, N.J. Turro, J. Phys. Chem. B 102 (1998) 5088.
[46] J. Seo, K.-Y. Cho, H. Han, Polym. Degrad. Stab. 74 (2001) 133.
[47] J. Diao, D.W. Hess, Thin Solid Films 483 (2005) 226.
[48] D. Losic, J.G. Shapter, J.J. Gooding, Langmuir 17 (2001) 3307.